ASME TURBOEXPO 2000
May 8-11, 2000, Munich Germany

2000-GT-107

ACTIVE CONTROL ANALYSIS FOR COMBUSTION-DRIVEN DYNAMIC INSTABILITIES IN GAS-TURBINE COMBUSTORS

M. A. Mawid & T. W. Park
Engineering Research and Analysis Company

B. Sekar
Turbine Engine Division
Air Force Research Laboratory
Wright-Patterson AFB, OH 45433

ABSTRACT

A one-dimensional combustor model has been used to simulate combustion-driven dynamic instabilities and their active control in a generic gas turbine combustor. The combustor model accounts for the unsteady heat release and viscous effects along with choked and open boundaries. Combustion is modeled by using global kinetics for JP-8 fuel. The active control methodology simulated in this study was based upon modulating the primary fuel injection rate. A sinusoidal functional form was implemented to pulse the fuel flow at various frequencies and amounts of pulsated fuel. The numerical results showed that the combustor unstable modes were captured and pressure limit cycle oscillations were attained for certain time lags between the instant of fuel-air mixture injection and heat release. The results also exhibited the effect of varying the time lag to damp out the instability. The simulations also showed that fuel pulsation with frequencies greater or less than the combustor resonant frequencies can suppress the unstable modes.

NOMENCLATURE

a^* = Reference speed of sound
D = Diffusion coefficient
K_0 = Reaction rate constant
k = Bulk modulus of the fluid
L = Combustor length
$\dot{m}$ = Fuel-air mixture injection rate
Pr_t = Turbulent Prandtl number, $\mu_t c_p / k_t$
p = Non-dimensional pressure, $\bar{p}/p^*$
p^* = Reference pressure
p' = Combustor pressure fluctuations
Q_{fh} = Heat transferred from/to the flameholder
q_0 = Heat of reaction
R = Non-dimensional reaction rate
Re^* = Reference Reynolds number, $\rho^* a^* L/\mu$
Sc_t = Turbulent Schmidt number, ν/D
T = Non-dimensional temperature, $\bar{T}/T^*$
T^* = Reference temperature
T_i = Non-dimensional temperature in the i^{th} numerical cell
T_i^{fh} = Non-dimensional temperature at the flameholder location
T_{ign} = Non-dimensional ignition temperature
t = Non-dimensional time, $\bar{t}/t^*$
t^* = Reference time, L/a^*
u = Non-dimensional axial velocity, $\bar{u}/a^*$
V = Volume of the fuel feed system
x = Non-dimensional distance, $\bar{x}/L$
y_i = Mass fraction of i^{th} species

Greek Letters

α = User specified constant in Eq. (7)
ε_t = Turbulent to laminar viscosity ratio, μ_t/μ

ϕ = Equivalence ratio

γ = Specific heat ratio, c_p/c_v

μ = Molecular viscosity

μ_t = Turbulent viscosity

ρ = Non-dimensional density, $\bar{\rho}/\rho^*$

ρ^* = Reference density

ω = Non-dimensional fuel pulsation frequency

Superscripts

* = Reference quantities

– = Dimensional quantities

Subscripts

o = Total quantities

INTRODUCTION

The Air Force Integrated High Performance Turbine Engine Technology (IHPTET) combustors must operate free of combustion-driven dynamic instabilities that could compromise the structural integrity of high performance engines. To double the thrust to weight ratio, as required for future high performance military engines, the combustor will be required to operate at much higher overall design equivalence ratios, P3 and T3 than the existing military aircraft engines combustors. In addition, weight reductions in the combustor, diffuser and fuel injectors can be only achieved through innovative integration and packaging of these components. Therefore, combustor, diffuser and fuel injectors must be designed in a manner that will lead to instability-free (or substantially damped instabilities) operation. Active combustion control techniques may also be implemented to damp instabilities. While the active control technology attempts to introduce an out of phase disturbance with the combustor pressure acoustics, the passive control technology requires a profound understanding of the various driving mechanisms such as air and fuel flows variations, unsteady heat release and their interaction that cause combustion instabilities.

Most existing combustors design databases lack a provision for predicting combustion-driven instabilities during the predesign and design phases. Currently, a need exists to predict and quantify combustion instabilities in high performance military combustors. Axial, tangential and radial instability modes may all develop in the combustors that could severely impact the engine performance and its structural integrity. Various approaches are presently used to predict combustion instabilities. These approaches range from one-dimensional linear stability-based [1-3], to one, two and three-dimensional non-linear-CFD-based [4-8]. Mohanraj et. al. [5] developed a one-dimensional combustor model using a heuristic mixing model along with a semi empirical open loop active controller. Quinn and Paxson [9] used a one-dimensional model to study thermo-acoustic instabilities in combustion systems. Other analytical models [10-11] based upon the unsteady-pressure wave equation in three-dimensions were also developed and calibrated/anchored to experimental results under controlled conditions such that extrapolation to other conditions can be performed.

Due to the limited data available on combustion-driven instability for gas turbine combustors, no consensus as to what approach should be used to predict instabilities during the diffuser/fuel injectors/combustor predesign and development stages yet exists. The primary objective of this study is to demonstrate the application of an unsteady one-dimensional combustor model for predicting the combustor's unstable modes and for investigating the effectiveness of the fuel flow modulation methodology to actively control and suppress the combustor's instabilities. The one-dimensional combustor model is computationally cost-effective and yet accounts for the most dominant physics causing instabilities in the axial direction. The model can, therefore, be used as a design tool, to predict the axial modes of instabilities in gas turbine combustors.

GOVERNING EQUATIONS

The combustor model numerically integrates the following governing differential equations for a calorically perfect gas. The governing equations are given below in non-dimensional form [9] as

$$\frac{\partial w}{\partial t} + \frac{\partial F(w)}{\partial x} = S \tag{1}$$

where the dependent vector w is given as

$$w = \begin{bmatrix} \rho \\ \rho u \\ \dfrac{p}{\gamma - 1} + \dfrac{\rho u^2}{2} \\ \rho\, y_i \end{bmatrix} \tag{2}$$

and the flux vector is given by

$$F = \begin{bmatrix} \rho u \\ \frac{p}{\gamma} + \rho u^2 \\ u\left(\frac{p}{\gamma - 1} + \frac{\rho u^2}{2}\right) \\ \rho\, u\, y_i \end{bmatrix} \tag{3}$$

The non-dimensionalization of pressure, p, temperature, T, density, ρ, and velocity, u has been obtained by using the reference quantities p^*, T^*, ρ^*, and a^*. The coordinate x has been scaled by the combustor length L. The time has been scaled using the sound wave transit time $t^* = L/a^*$. The heat of combustion q_0 is assumed to be a constant. The ratio of specific heats is denoted by γ.

The non-dimensional form of the equation of state is given as

$$p = \rho T \tag{4}$$

The source vector in Eq. (1) is given as

$$S = \begin{bmatrix} 0 \\ \frac{\partial}{\partial x}\left(\frac{\varepsilon_t}{\mathrm{Re}^*}\left(\frac{\partial u}{\partial x}\right)\right) + \sigma_2 u|\rho u|^{0.75} \\ \frac{\partial}{\partial x}\left(\frac{\varepsilon_t}{\mathrm{Re}^*}\frac{\partial}{\partial x}\left(\frac{u^2}{2} + \frac{p}{(\gamma-1)\,\mathrm{Pr}_t}\right)\right) + q_0 R + Q_{fh} \\ \frac{\partial}{\partial x}\left(\frac{\varepsilon_t}{\mathrm{Re}^*\, Sc_t}\left(\frac{\partial y_i}{\partial x}\right)\right) - R \end{bmatrix} \tag{5}$$

Equation (5) contains contributions from the reaction, turbulent eddy diffusion, wall viscous forces, and flameholder heat transfer. The Reynolds number, Re^* is defined as $\rho^* a^* L/\mu$. The turbulent viscosity ratio, ε_t is defined as the ratio of turbulent to molecular viscosity, μ_t/μ. R is the reaction rate, defined below. Pr_t and Sc_t are the turbulent Prandtl and Schmidt numbers respectively.

Combustion Model

The combustion model employed in this study was based upon a single-step chemistry reaction scheme. The non-dimensional reaction rate has the form:

$$R = K_0 \rho\, y_f\, y_{o_2} \begin{Bmatrix} 1 - \left(T_{ign}/T_i\right) & ; T_i > T_{ign} \\ 0 & ; T_i < T_{ign} \end{Bmatrix} \tag{6}$$

where K_0 is the reaction rate constant, T_{ign} is the ignition temperature and T_i is the temperature in the i^{th} numerical cell. Due to the one-dimensionality of the combustor model, flame holding is accomplished by a 10% change of the ε_t over the combustor length from zero to a specified value.

Flameholder Heat Transfer

The term Q_{fh} in Eq. (5) is represented by a simple algebraic expression

$$Q_{fh} = \alpha(0.9T_{ign} - T_i^{fh}) \tag{7}$$

where α is a user specified constant, $0.9T_{ign}$ represent the assumed temperature of the flameholder to or from which heat may be transferred, and T_i^{fh} is the (computed) gas temperature at the flameholder location. Note that when this model is used, energy is not strictly conserved in the system. That is, energy may be brought into or taken from the system by this term. T_{ign} is assumed to be constant, since the flame response time scale is much smaller than that of the flameholder wall temperature.

Numerical Methodology

The combustor model numerically integrates the above equations of motion using a very simple, second-order MacCormack scheme. Artificial viscosity has been added in order to damp non-physical oscillations in the vicinity of strong gradients such as those brought about by the combustion process [12-15]. A number of grid independent studies were conducted to ensure that physical instability would not be damped [15]. In the current study, the grid size was $\Delta x = 0.005$ mm for which the results were very much grid-independent, as will be shown in the results.

Boundary Conditions

Boundary conditions may be imposed as either partially opened, fully open, or choked inflow (e.g. constant mass flux) ends. In either case the model anticipates the flow direction and applies appropriate (e.g. well posed) states. If the flow is outward from the computing domain, only the static pressure is imposed. The remaining information, density, velocity, and

mass fraction are obtained from the interior of the computational domain. If the flow is inward, total pressure and temperature, and mass fraction are imposed. The remaining unknown quantities (velocity, static temperature and pressure) are obtained through an iteration procedure by using isentropic relations for static and total temperature and pressure. In other words, the velocity is first obtained by using $\partial u/\partial x = 0$ at the exit. Then, the static temperature is obtained iteratively through the relation $T_o/T = 1 + 0.5(\gamma - 1)u^2/(\gamma RT)$. Finally, the static pressure is obtained through p_o/p_t relation.

RESULTS

Numerical results have been obtained to demonstrate the applicability of the unsteady one-dimensional combustor model to predict combustion-driven instability in a generic gas turbine combustor. Figure 1 shows the schematic of the combustor geometry investigated in this study. Fully premixed fuel-air mixture was assumed at the inlet of the combustor. The fuel type used was JP-8. Combustor model constants used in this study are given in Table 1. As indicated earlier, two different types of exit boundary conditions were implemented in the combustor model, namely, full open and choked. In this preliminary study, only the open exit boundary condition was used. The boundary condition imposed at the exit corresponds to a non-dimensional pressure value of unity. In fact, the reference pressure in this study was assumed to be equal to the back pressure. Due to the one-dimensionality of the combustor model, the effects of the swirl velocity component was accounted for by using a 1.1 % reduction in the static pressure at the combustor inlet.

The combustor model assumes that a constant fuel-air flux can be specified at the inlet in the absence of combustor pressure acoustics. This condition is essentially a choked boundary in which the effect of the downstream pressure acoustics are not sensed upstream of the inlet. However, a choked inlet condition would lead to stable combustion as the computations showed. The dependence of the inlet fuel-air mixture flux upon the combustor pressure should, therefore, be determined through a fuel injection system model. Since the current study assumes the computational domain to start at the backward facing step, a lumped-element parameter model for the fuel injectors/swirlers was considered.

$$\dot{m}_2 = \dot{m}_1 - \frac{\rho V}{k}\frac{dp'}{dt} \qquad (8)$$

Equation (8) expresses the dependence of the fuel-air flow rate at the inlet of the combustor, $\dot{m}_2$, on the combustor pressure oscillations p'. The fuel-air mixture mass flow rate $\dot{m}_1$ is a constant. Equation (8) also implies that as the combustor pressure oscillation $p' \to 0$, $\dot{m}_2 = \dot{m}_1$ and a constant fuel-air mixture flow rate is then imposed at the combustor inlet.

The location of the fuel injection and the time required for the fuel-air mixture to react are very critical parameters for either driving or damping the instabilities [6,7]. The time delay between the instant of fuel injection and the instant of heat release is primarily governed by the mixing and chemical kinetic times. To account for this time delay, various estimations of this time delay were made based on the location of the fuel injector and chemical times for different equivalence ratios (i.e., ϕ = 0.5 - 0.8), initial temperatures (i.e., T_{inlet} = 700 - 900 K) and Damkohler numbers (Da = 1.0 - 100). The time delay was then used in the combustor model to determine the instant at which the fuel-air mixture, $\dot{m}_1$, is injected. The resultant mixture injection was therefore shifted in time by an amount equal to the time delay (i.e., injection time = $t \pm \delta t$) and $\dot{m}_1(t \pm \delta t)$ is injected.

Figures 2 and 3 show the combustor limit cycle pressure oscillations and the corresponding heat release in non-dimensional form and for a time delay of 1.97×10^{-3} s and at a non-dimensional location x = 0.8. This value of the time delay was found to produce the largest amplitude of the pressure oscillations. The cycle limit pressure oscillations have a non-dimensional period of approximately 0.9 (or 3.6×10^{-3} s) and a corresponding non-dimensional frequency of 1.11 (or 278 Hz). It can also be seen that these strong oscillations have shock waves characteristics, which indicate that these are a strong longitudinal instability of the fundamental mode 278 Hz. In addition, a close examination of the limit cycle pressure oscillations and that of the heat release fluctuations clearly exhibits the phase relationship between the heat release and the pressure oscillations. Pressure and heat release oscillations were predicted to be in phase and thus satisfy Rayleigh's criterion for driving instability.

Figure 4 shows the pressure field oscillations for a time delay of 3.8×10^{-3} s which is equal to 1.97×10^{-3} + half the limit cycle period shown in Fig. 2. It is clearly seen that the strong limit cycle oscillations of Fig. 2 have been substantially damped, consistent with the time lag theory of Crocco [16]. This demonstrates the capability of the combustor model to simulate non-linear behavior. Additional simulations were carried out to substantiate the time delay effect and the results were all consistent. It should be mentioned that when calculations were made for constant fuel-air mixture mass flow rate (time delay and p' are set equal to zero), a steady-state combustion was predicted.

To further demonstrate the ability of the combustor model to carry out active control calculations, the combustor response to fuel flow modulation as a means to actively control instability was predicted. The fuel injection was pulsed sinusoidally at different frequencies and amounts. The predictions represent the open loop response of the controlled combustor as shown in Fig.1. Note here that no phase shift and controller gain were used in the current study. The inlet condition for the open loop calculations was set to be a constant fuel-air mixture flux with various time delays (i.e., non-choked inlet) and the exit condition was also open with a specified non-dimensional pressure of unity. The combustor length was also kept the same to ensure that the combustor resonant frequencies are considerably higher than the fuel pulsation frequencies. The amplitude of the amount of fuel pulsed was varied between 2% to 10% of the total primary fuel injection rate and the combustor response was studied.

Figures 5-8 show the predicted combustor response in terms of the non-dimensional pressure, temperature, velocity and primary fuel mass fraction for a time delay of 1.97×10^{-3} s and at the non-dimensional location $x = 0.8$. The non-dimensional fuel pulsation frequency ω was 0.6 (i.e., $\omega = 150$ Hz) and the non-dimensional magnitude A was 2% of the primary fuel rate. The sinusoidal fuel pulsation was turned on at the start of the computations (i.e., after one computational time step for convergence and code stability). The results clearly show that significant damping of the pressure, temperature and velocity oscillations occurred. In particular, it can be seen that the pressure initially increases due to the rapid rise in the temperature and then it is followed by a period over which the pressure oscillates and finally the oscillations damp out. This behavior is also reflected in temperature and velocity fields.

Figures 9 and 10 show the non-dimensional pressure and temperature in the combustor for A = 10% of the primary fuel rate and for the same conditions as in Figs. 5 through 8. It can be seen that increasing the amount of pulsed fuel does not always result in more damping. In fact, the amplitude of the final oscillations appear to be somewhat greater than that of the previous case, for A = 2%. However, the increase in the oscillation magnitude is not significant.

To further study the effect of fuel pulsation on the combustor response, the fuel pulsation was turned on after the limit cycle pressure oscillations were reached for the case presented in Figs. 2 and 3. The combustor response predictions are shown in Figs. 11-13. It is clearly demonstrated that if the fuel is pulsed after the system has reached a limit cycle, the decrease in the amplitude of the pressure oscillations appears to be limited and never goes to zero as the computations revealed. The reason for this behavior may be attributed to the inability of pulsed fuel to produce a secondary heat release oscillation of sufficient amplitude and be completely out of phase with the strong limit cycle pressure oscillations. This can further be seen in Fig. 11 where the heat release fluctuations are not entirely out of phase with the pressure oscillations. It should also be indicated that a similar behavior was seen [5], when an active control was turned on after the system has reached the limit cycle behavior. This is indicative of the unsatisfactory performance of fuel pulsation to control instability in the limit cycle regime. Multiple fuel pulsation frequencies based on multiple pressure modes sensed in the combustor will be required to damp non-linear instabilities, which will be investigated in the near future.

CONCLUSION

A one-dimensional combustor model was used to study active control of combustion-driven instabilities in a generic gas turbine combustor. The numerical predictions clearly demonstrated the effect of the time delay between the instant of fuel injection and heat release. By varying this time delay, damping or driving of the instability may occur. The predictions showed that there existed a single time delay value for the combustor geometry considered here and for which strong instability can set out and is manifested by a limit cycle behavior. The analysis also showed that these strong pressure oscillations can be damped out by changing the delay time by some factor multiplied by the oscillation period.

The combustor model was also used to investigate the combustor response to fuel flow pulsation to control instability. The results clearly demonstrated that for fuel pulsation to be effective in controlling instability, the fuel modulation must be turned on at the start of the engine. Moreover, the results indicated that multiple frequency-based fuel pulsation might be required to damp out strong shock wave type instability oscillations.

Finally, it should be mentioned that the combustor model developed here is a very useful predictive tool that can be used during the predesign and design stages to predict the dynamic instability characteristics of new combustor designs in a very efficient manner. This computer model can also be used to support experimental work for parametric studies.

ACKNOWLEDGMENTS

The authors would like to thank Dr. Paxson from NASA Glenn Research Center for the technical discussion and providing us with the original baseline code.

REFERENCES

1. Darling, D., Radhakrishnan, K., Oyediran, A., and Cowan, E., "Combustion-Acoustic Stability Analysis for Premixed Gas Turbine Combustors," NASA TM 107024.
2. Bloxsidge, G. J., Dowling, A. P., and Langhorne, P. J., "Reheat Buzz: an Acoustically Coupled Combustion Instability. Part 2. Theory," *J. Fluid Mech.*, Vol. 193, pp. 445-473, 1988.
3. Bloxsidge, G. J., Dowling, A. P., and Langhorne, P. J., "Active Control of Reheat Buzz," *AIAA Journal*, Vol. 26, No. 7, pp. 783-790, 1988.
4. Shyy, W. and Udaykumar, "Numerical Simulation of Thermo-Acoustic Effect on Longitudinal Combustion Instabilities," 26th JPC, AIAA 90-2065, 1990.
5. Mohanraj, R. and Zinn, B. T., "Numerical Study of the Performance of Active Control Systems for Combustion Instabilities," 36th JPC, AIAA 98-0356, 1998.
6. Smith, C.E., and Leonard, A., D. "CFD Modeling of Combustion Instability in Premixed Axisymmetric Combustors," ASME Paper 97-GT-305, 1997.
7. Habiballah, M. and Dubois, I., "Numerical Analysis of Engine Instability," 31st JPC, AIAA 95-37213, 1995.
8. Kim, Y. M., Chen, C. P., Ziebarth, J. P., and Chen, Y. S., "Prediction of High Frequency Combustion Instability In Liquid Propellant Engines," 28th JPC, AIAA 92-3763, 1992.
9. Quinn, D., D and Paxson, D. E., "A Simplified Model for the Investigation of Acoustically Driven Combustion Instability," 34th JPC, AIAA 98-3764, 1998.
10. Hsiao, G., Pandalai, R., Hura, H., and Mongia, H. C., "Combustion Dynamic Modeling for Gas Turbine Engines," 34th JPC, AIAA 98-3380, 1998.
11. Yang, V., and Anderson, W., "Liquid Rocket Engine Combustion instability," *Progress in Astronauts and Aeronautics*, Vol. 169, 1995.
12. Paxson, D. E., "A General Numerical Model for Wave Rotor Analysis," NASA TM 105740, July 1992.
13. Paxson, D. E., "An Improved Numerical Model for Wave Rotor Design and Analysis," AIAA Paper 93-0482, January 1993, also NASA TM 105915.
14. Paxson, D. E., "A Comparison Between Numerically Modeled and Experimentally Measured Loss Mechanisms in Wave Rotors," *AIAA Journal of Propulsion and Power*, Vol. 11, No. 5, 1995, pp. 908-914, also NASA TM 106279.
15. Nalim, R. M. and Paxson, D. E., "A Numerical Investigation of Premixed Combustion in Wave Rotors," *ASME Journal of Engineering for Gas Turbines and Power*, Vol. 119, No. 3, 1997, pp. 668-675, also ASME Paper 96-GT-116, June, 1996, also, NASA TM 107242.
16. Crocco, L. and Cheng, S.-I., "Theory of Combustion Process Instability in Liquid Rocket Engines," IL, Moscow, 1958, pp. 59-69.

Table 1

Model Constants	
γ	1.37
ε_t	0.002
Sc_t	1.0
Pr_t	1.0
T_{ign}	1.25

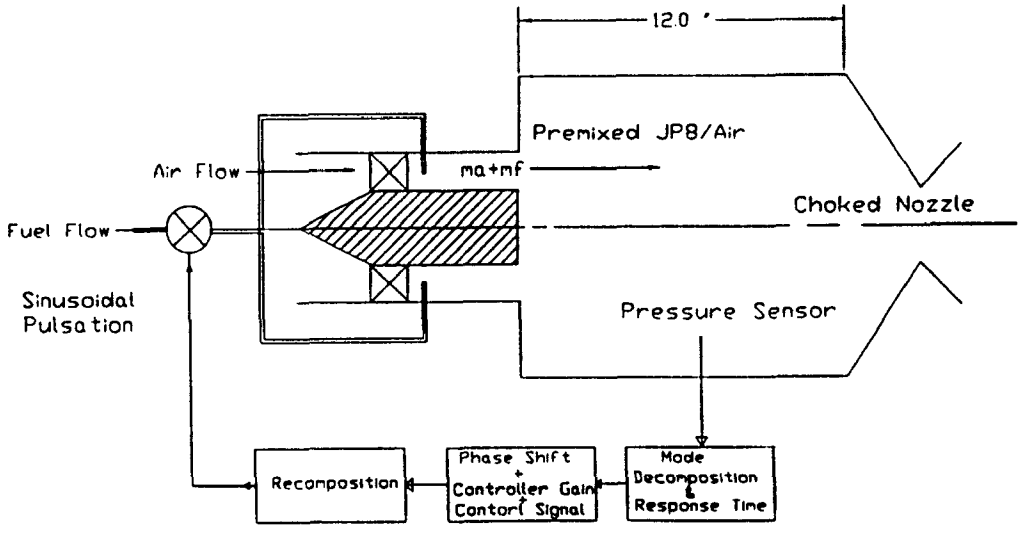

Fig. 1 A Schematic of the Combustor and Control System.

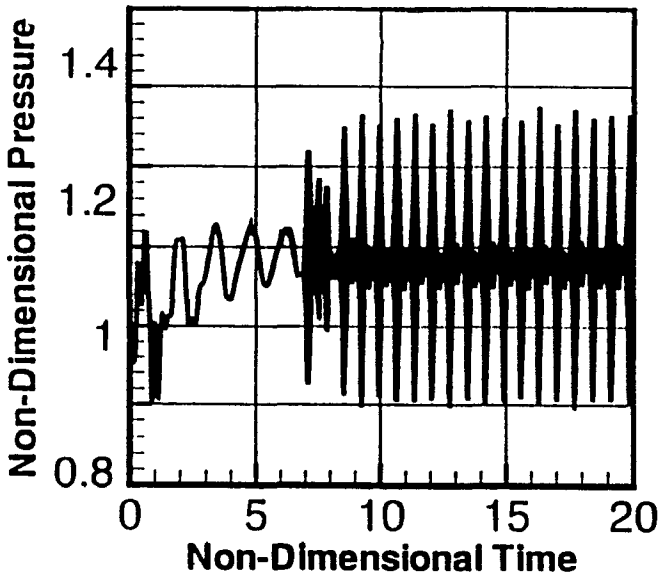

Fig. 2 Limit Cycle Pressure Oscillations for a Time Delay $\delta t = 1.97 \times 10^{-3}$ s.

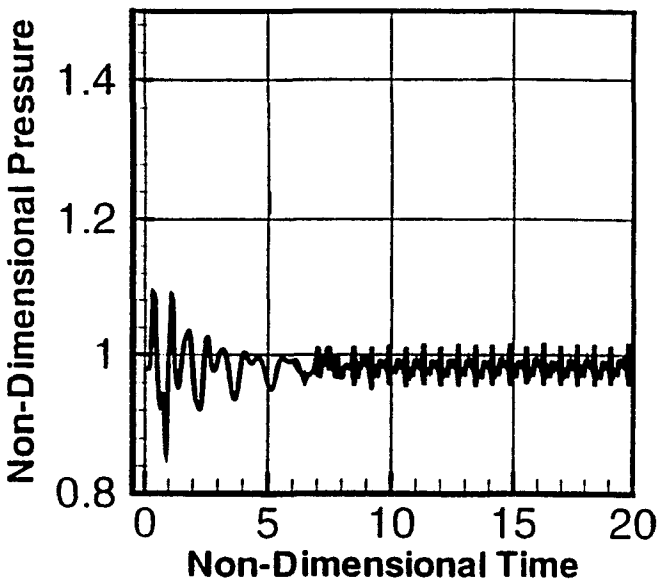

Fig. 4 Effect of Time delay on the Limit Cycle Pressure Oscillations for a Time Delay $\delta t = 1.97 \times 10^{-3} + 1.8 \times 10^{-3}$ s.

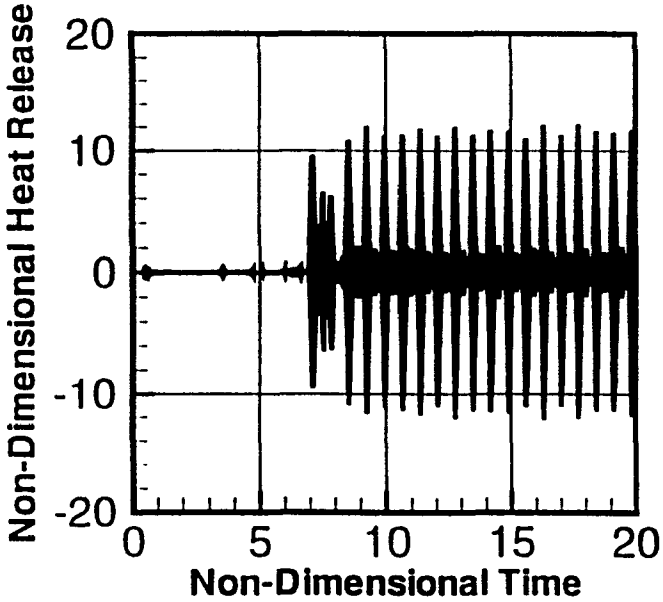

Fig. 3 Non-Dimensional Limit Cycle Heat Release Oscillations Corresponding to $\delta t = 1.97 \times 10^{-3}$ s.

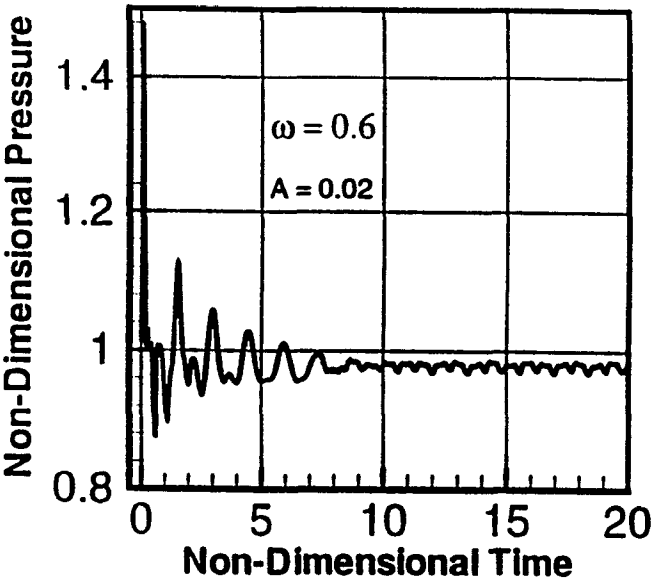

Fig. 5 Effect of Fuel Modulation on the Pressure Oscillations for Concurrent Primary and Pulsed Fuel Injection.

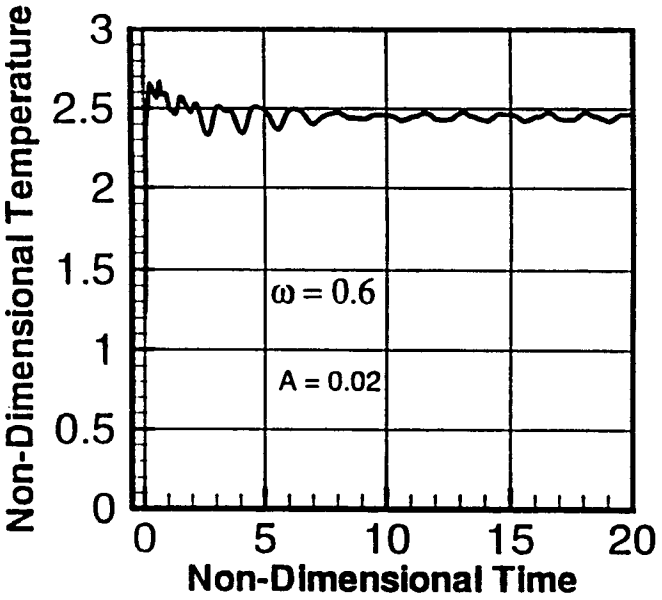

Fig. 6 Effect of Fuel Modulation on the Temperature Oscillations for Concurrent Primary and Pulsed Fuel Injection.

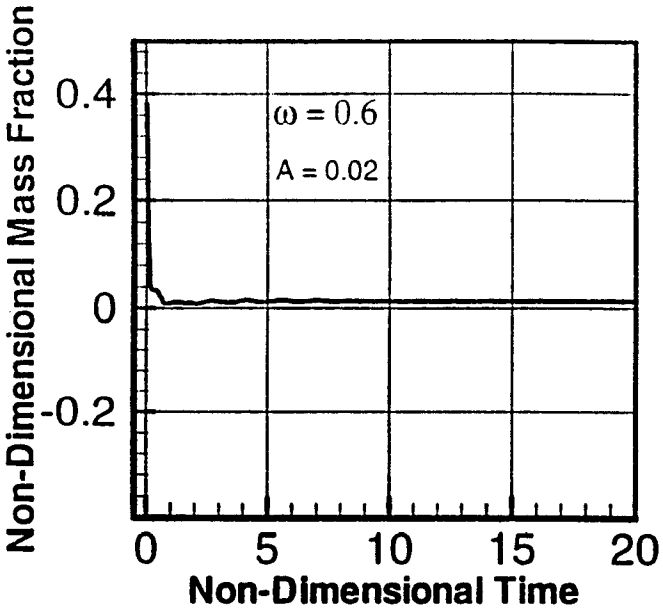

Fig. 8 Effect of Fuel Modulation on the Fuel Concentration Oscillations for Concurrent Primary and Pulsed Fuel Injection.

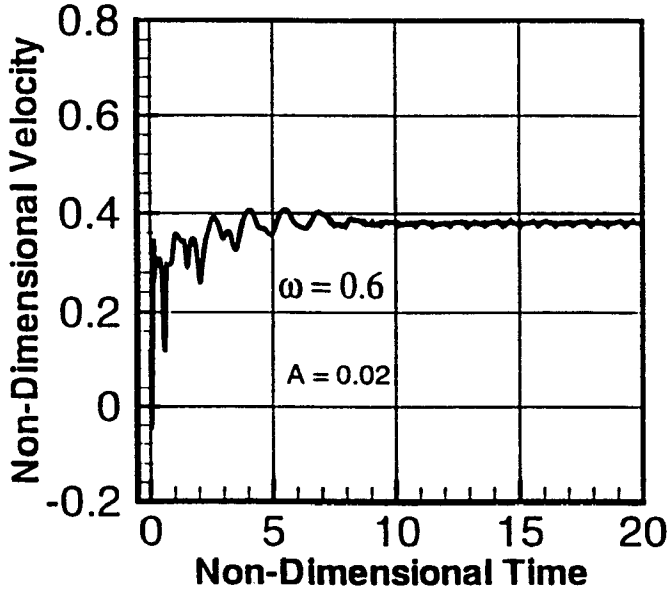

Fig. 7 Effect of Fuel Modulation on the Velocity Oscillations for Concurrent Primary and Pulsed Fuel Injection.

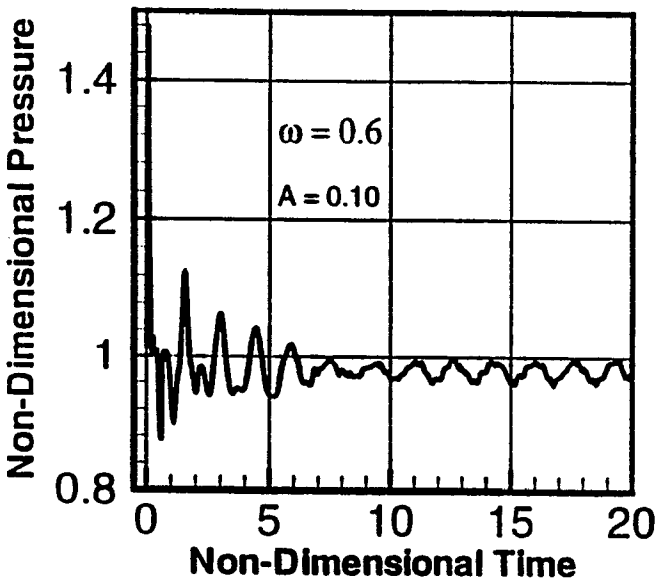

Fig. 9 Effect of the Amount of Fuel Modulation on the Pressure Oscillations for Concurrent Primary and Pulsed Fuel Injection.

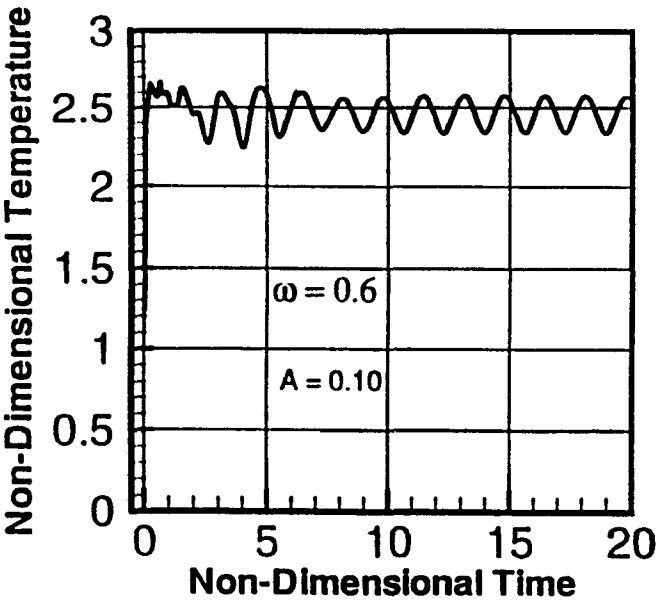

Fig. 10 Effect of the Amount of Fuel Modulation on the Temperature Oscillations for Concurrent Primary and Pulsed Fuel Injection.

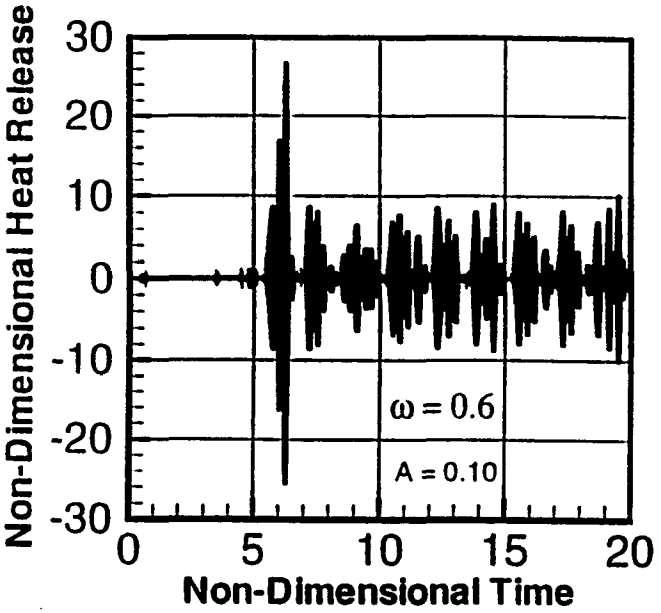

Fig. 12 Effect of Fuel Modulation on the Limit Cycle Heat Release Oscillations for Non-Concurrent Primary and Pulsed Fuel Injection.

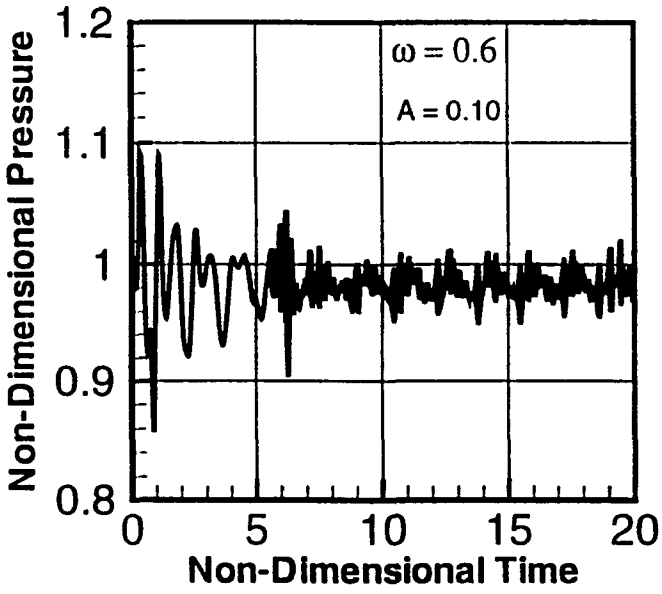

Fig. 11 Effect of Fuel Modulation on the Limit Cycle Pressure Oscillations for Non-Concurrent Primary and Pulsed Fuel Injection.

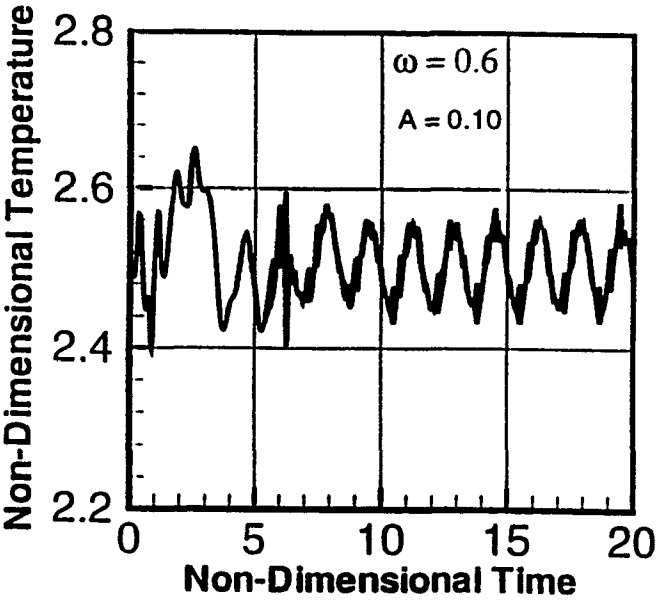

Fig. 13 Effect of Fuel Modulation on the Limit Cycle Temperature Oscillations for Non-Concurrent Primary and Pulsed Fuel Injection